Synchronized Assembly of Gold Nanoparticles Driven by a Dynamic DNA-Fueled Molecular Machine

ARTICLE *in* JOURNAL OF THE AMERICAN CHEMICAL SOCIETY · JUNE 2012

Impact Factor: 12.11 · DOI: 10.1021/ja304746k · Source: PubMed

2 AUTHORS:

Tingjie Song
University of Science and Technology of China
8 PUBLICATIONS **53** CITATIONS
SEE PROFILE

Haojun Liang
University of Science and Technology of China
153 PUBLICATIONS **2,256** CITATIONS
SEE PROFILE

JACS
JOURNAL OF THE AMERICAN CHEMICAL SOCIETY
Communication
pubs.acs.org/JACS

Synchronized Assembly of Gold Nanoparticles Driven by a Dynamic DNA-Fueled Molecular Machine

Tingjie Song[†] and Haojun Liang*[,†,‡]

[†]CAS Key Laboratory of Soft Matter Chemistry, Department of Polymer Science and Engineering, University of Science and Technology of China, Hefei, Anhui 230026, P. R. China

[‡]Hefei National Laboratory for Physical Sciences at the Microscale, University of Science and Technology of China, Hefei, Anhui 230026, P. R. China

Supporting Information

ABSTRACT: A strategy for gold nanoparticle (AuNP) assembly driven by a dynamic DNA-fueled molecular machine is revealed here. In this machine, the aggregation of DNA-functionalized AuNPs is regulated by a series of toehold-mediated strand displacement reactions of DNA. The aggregation rate of the AuNPs can be regulated by controlling the amount of oligonucleotide catalyst. The versatility of the dynamic DNA-fueled molecular machine in the construction of two-component "OR" and "AND" logic gates has been demonstrated. This newly established strategy may find broad potential applications in terms of building up an "interface" that allows the combination of the strand displacement-based characteristic of DNA with the distinct assembly properties of inorganic nanoparticles, ultimately leading to the fabrication of a wide range of complex multicomponent devices and architectures.

In the mid-1990s, two leading groups[1,2] pioneered the utilization of oligonucleotides as noncovalent linkers for mediating the interaction potential between gold nanoparticles (AuNPs) as well as directing the assembly of DNA-functionalized gold nanoparticles (DNA–AuNPs).[3] Since then, the combination of the powerful programmable capability of nucleic acids and the distinguished assembly performance of AuNPs has paved an exciting way leading to the fabrication of nanomaterials possessing the hybridized properties of both organic DNA and inorganic metal colloids. Because of their unique optical and catalytic properties, DNA–AuNPs have now found a number of practical applications in the fields of biodiagnostics, medicine, and biosensors in terms of colorimetric-based detection,[4] electronic-based detection,[5] scanometric-based detection,[6] Raman-based detection,[7] and antisense gene control.[8]

Of late, the assembly of DNA–AuNP structures consisting of amorphous face-centered-cubic or body-centered-cubic crystals has been successfully regulated by tailoring the length of the oligonucleotide linkers.[9,10] The position and arrangement of AuNPs in space were aptly mediated via DNA hybridization, allowing AuNPs to assemble into two-dimensional geometric patterns.[11−13] The kinetics and pathways of the assembly were controlled by adjusting the conformation of the oligonucleotides on the surface of the AuNPs.[14,15]

On the other hand, toehold-mediated DNA strand displacement, a concept pioneered by Yurke et al.[16] to build dynamic DNA-fueled molecular machines, occurs when a single-stranded DNA on a double-stranded complex is displaced by another single-stranded DNA with the help of a short sequence of contiguous bases (called a toehold). Recently, this concept has been used to build a nanomachine that drives the switching of DNA motifs between two topological structures,[17,18] to build molecular gears that could continuously roll against each other,[19] to trigger the assembly of two stable species of DNA coexisting in solution,[20] to control the assembly and disassembly of DNA hairpin motifs,[21] and to build an autonomous polymerization motor powered by DNA hybridization.[22] Most notably, toehold-mediated strand displacement has been applied to the construction of entropy-driven catalytic reactions,[23] chemical reaction networks,[24] synthetic transcriptional clocks,[25] and digital logic circuits (culminating in a four-bit square-root circuit).[26] In these systems, oligonucleotide chains act as catalysts or as inputs that fuel the DNA-based molecular machine by a series of toehold strand displacement reactions in a "geometry-free-like" network.

Despite their success in the above two fields, previous studies of the assembly of AuNPs have primarily used an assembly strategy in which the DNA–AuNPs and oligonucleotide linkers are simultaneously introduced into the reaction system, which we call the "direct linker addition" strategy. In contrast, a DNA-machine-driven strategy, in which an oligonucleotide, possibly released from a potential upstream circuit, plays the role of triggering and driving a DNA-fueled molecular machine to mediate the assembly of AuNPs, has not been developed to date. On the other hand, current applications of toehold-mediated DNA strand displacement to molecular machines have been focused on pure DNA systems. We anticipate the DNA chains conjugated with inorganic nanoparticles acting as fuel in a molecular machine may bring some novelty to the construction of a molecular machine.

In the present work, the assembly of AuNPs driven by a dynamic DNA-fueled molecular machine was examined. The assembly into explicit geometrical structures of DNA–AuNPs was triggered and mediated via a series of strand displacement reactions that occur in geometry-free-like networks. The present strategy involved the design and syntheses of five

Received: May 16, 2012
Published: June 16, 2012

dx.doi.org/10.1021/ja304746k | J. Am. Chem. Soc. 2012, 134, 10803−10806

types of oligonucleotides [see Table S1 in the Supporting Information (SI)]. Two types of DNA–AuNPs were first prepared by functionalizing the surface of 13 nm diameter AuNPs with one of two oligonucleotides, oligomer-1 or oligomer-2. To accomplish the DNA-machine-driven assembly, the linker-oligomers deliberately were not added directly into the solution, as their presence might cause aggregation of the two types of DNA–AuNPs via hybridization of the complementary domains in the two terminal ends of the linker-oligomers with those grafted on the surface of the AuNPs. Instead, a segment of the linker-oligomer was hybridized with the protector-oligomer to form a complex that prevented the sticky end of the linker-oligomer from unintentionally reacting with sequences grafted on the surface of the AuNPs (Figure 1). It is important to realize that

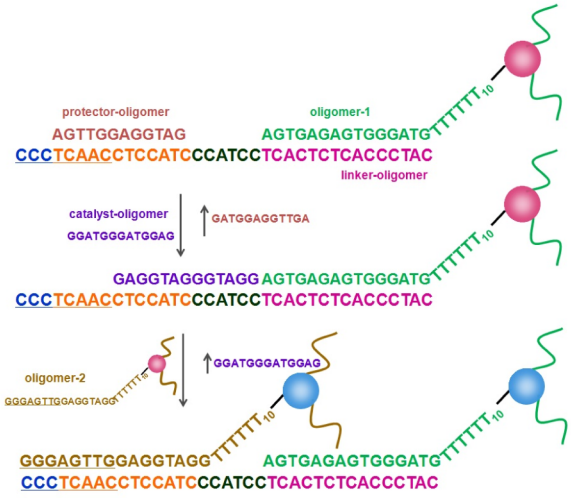

Figure 1. Graphical representation of the dynamic DNA-fueled molecular machine strategy and the mechanism of DNA–AuNP assembly.

aggregation in the system containing the two kinds of DNA–AuNPs and the complex must be avoided, allowing the system to remain sufficiently stable for a long time. Introduction of small quantities of catalyst-oligomer triggered the running of the DNA-fueled molecular machine with the assistance of a series of toehold-mediated DNA strand displacement reactions, ultimately resulting in linking of the two types of DNA–AuNPs. The details of the reaction are as follows (Figure 1): Briefly, the protector-oligomer on the complex was first displaced by the catalyst-oligomer through a toehold-mediated strand displacement, generating a new complex with a duplex of the linker-oligomer and catalyst-oligomer. Subsequently, oligomer-2 grafted on an AuNP displaced the catalyst-oligomer through another toehold-mediated DNA strand displacement reaction.The whole cycle resulted in the cross-linking of the two types of AuNPs via the duplex formation of oligomer-2 and linker-oligomer and was accompanied by release of the catalyst-oligomer into the solution. This nonconsumption of the catalyst-oligomer during these reactions reflects the behavior of a true catalyst. The DNA machine ran continuously until all of the DNA–AuNPs were cross-linked to form larger clusters, which resulted in visible deposits in the reaction mixture (Figure 2 inset and Figure S2 in the SI).

It is reasonable to believe that the toehold length of the complex formed by the linker-oligomer and the catalyst-oligomer should have an important effect on the rate of the catalyst-oligomer displacement by the oligomer-2 grafted on the AuNPs. The experimental results indicated that only when the toehold was eight bases long was the displacement rate suitable for the reaction to run (Figure 2). This behavior was

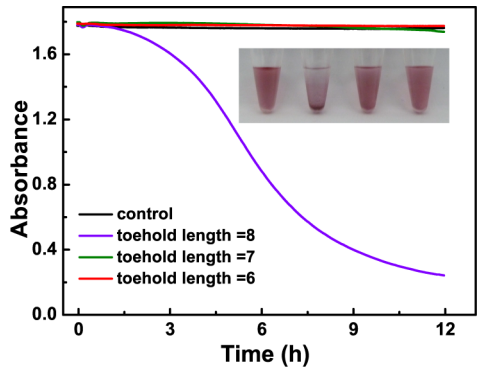

Figure 2. Kinetics of DNA–AuNP assembly with the complexes of the linker-oligomer and catalyst-oligomer having varied toehold lengths, monitored by absorbance at 520 nm. The inset panel shows the color change after 12 h for (from left to right) the control system without catalyst-oligomer and the systems with eight-, seven-, and six-base toeholds. [DNA–AuNP] = 3.5 nM, [complex] = 75 nM, [catalyst-oligomer] = 37.5 nM.

different from that observed in pure DNA systems, where a five-base toehold was enough to give a sufficiently high rate of the toehold-mediated stand displacement reaction.[27] The reason for this difference might arise from the steric hindrance and surface charge of the AuNP. Hence, the eight-base toehold was used in the following observations. Use of an eight-base toehold would not totally cover the 5′ half of the linker-oligomer; instead, three bases would be left uncovered upon formation of the complex of the linker-oligomer and the protector-oligomer (Figure 1). This might guarantee a higher reaction rate when the protector-oligomer is displaced by the catalyst-oligomer.

In practical applications, both a high aggregation rate of DNA–AuNPs and a low detection limit of DNA are desired. Thus, tests were performed to ensure that these two characteristics were exhibited at acceptable levels using the present DNA-machine-driven assembly strategy in comparison with the well-established direct linker addition strategy. After a number of tests, a suitable DNA–AuNP:DNA–AuNP:linker-oligomer molar ratio of 1:1:21 was selected for the direct linker addition strategy. In the subsequent experiments using the DNA-machine-driven assembly strategy, the same 1:1:21 molar ratio of the two DNA–AuNPs and the complex (composed of the linker-oligomer and protector-oligomer) was used to ensure that the amount of linker-oligomer would be consistent with that used in the assembly via direct linker addition. The aggregation of DNA–AuNPs was monitored via time-resolved UV–vis absorption spectroscopy at 520 nm (Figure 3) and color detection (Figure S2). Interestingly, when the amount of catalyst-oligomer added into the solution increased to 12% of the amount of linker-oligomer, the DNA–AuNPs showed an aggregation rate comparable to that of the direct linker addition strategy. This indeed ensured a time scale and detection limit comparable to those of the direct linker addition strategy, which would be particularly important in the future application of the DNA-machine-driven assembly scheme, especially in the area of

dx.doi.org/10.1021/ja304746k | J. Am. Chem. Soc. 2012, 134, 10803–10806

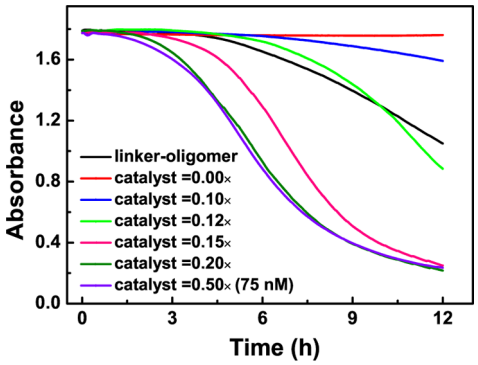

Figure 3. Kinetics of DNA–AuNP assembly with varied catalyst-oligomer concentrations. [DNA–AuNP] = 3.5 nM, [linker-oligomer] = [complex] = 75 nM.

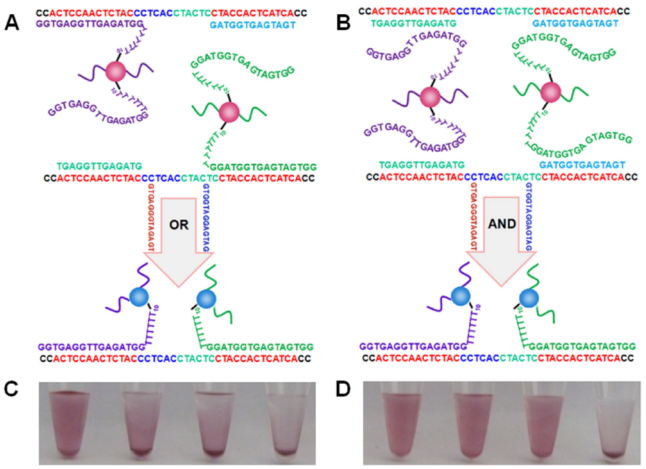

Figure 4. Two-component logic gates. [DNA–NP1] = [DNA–NP2] = 2.5 nM, [L-catalyst-1] = [L-catalyst-2] = 21 nM. (A, C) The "OR" logic gate includes two types of complexes, each at a concentration of 21 nM. (B, D) The "AND" logic gates includes one type of complex at a concentration of 42 nM. The colors from left to right in the panels of C and D represent addition of no catalyst chain, L-catalyst-1, L-catalyst-2, and both catalyst chains.

molecular diagnostics. Furthermore, these studies showed that the aggregation rate of DNA–AuNPs could be mediated and synchronized by controlling the amount of catalyst-oligomer. The optimal quantity of the catalyst-oligomer was 10–20% of the concentration of the linker-oligomer (Figure 3). While exceeding the upper limit did not further accelerate the reaction, using less than the lower limit led to intolerably slow reactions.

As indicated above, these DNA–AuNPs may find applications as probes in molecular diagnostics.[4] Toward this aim, the power of the assembly scheme was demonstrated by building DNA-based logic gates, which are currently being studied for genotypic assay development. To build the two-component "OR" and "AND" logic gates, two types of DNA–AuNPs (i.e., DNA–NP1 and DNA–NP2) were prepared by functionalizing the AuNPs with two sequences of the oligonucleotides, L-oligomer-1 and L-oligomer-2 (see Table S2). To build the OR gate, two types of complexes, L-linker + L-protector-1 and L-linker + L-protector-2 were prepared, in which one of two terminal ends of the L-linker was covered with its complementary sequence. One or both of L-catalyst-1 and L-catalyst-2 were subsequently added into the solution containing the mixture of the two protector-linker complexes and the two types of DNA–AuNPs, triggering aggregation of the DNA–AuNPs and resulting in the construction of the OR gate (Figure 4A,C). To construct the AND gate, a complex in which both terminal ends of the L-linker were covered with L-protector-1 and L-protector-2 was prepared. This was done to ensure that DNA–AuNP aggregation could be trigged only if both catalysts, L-catalyst-1 and L-catalyst-2, were present in the solution containing the two types of DNA–AuNPs and the complex (Figure 4B,D).

In this study, the capabilities of the DNA-based molecular machine in driving the assembly of DNA–AuNPs have been demonstrated. This machine provides an applicable strategy for building up an "interface" that allows the incorporation of the strand displacement-based characteristic of DNA into the assembly of inorganic nanoparticles. This strategy thus facilitates the coupling of the programmable feature of DNA with the distinguished electrical, optical, and catalytic properties of inorganic nanoparticles. The strategy has been successfully exemplified in the construction of two-component OR and AND logic gates, further confirming its advantages for engineering DNA–AuNP devices. This methodology can be applied for the construction of more complicated systems. For instance, the surface of the AuNPs could be functionalized with multiple-component DNA,[28,29] which would enable the construction of multiple-component logic gates for multiplexed DNA detection. Alternatively, the oligonucleotide chains acting as catalysts in this system could be released from upper-layer circuits and cascades to trigger the aggregation of AuNPs. This could be applied as an output indicator of the upper-layer circuit in colorimetric sensing and amplification. Thus, more complex and robust machines may potentially be constructed directly using this hybridization system, which may aid in new discoveries. Finally, this strategy can easily be extended to other inorganic nanoparticle systems with well-established coordination chemistries (e.g., Ag, Pt, CdSe, and CdS). The use of inorganic, anisotropic building blocks in our system may produce more attractive DNA–inorganic hybridization machines.[30–32]

■ ASSOCIATED CONTENT

Ⓢ Supporting Information

Description of experimental methods and analytical measurements. This material is available free of charge via the Internet at http://pubs.acs.org.

■ AUTHOR INFORMATION

Corresponding Author

hjliang@ustc.edu.cn

Notes

The authors declare no competing financial interest.

■ ACKNOWLEDGMENTS

This work was supported by the National Natural Science Foundation of China (Grants 20934004 and 91127046) and the National Basic Research Program of China (NBRPC) (Grants 2012CB821500 and 2010CB934500).

■ REFERENCES

(1) Mirkin, C. A.; Letsinger, R. L.; Mucic, R. C.; Storhoff, J. J. *Nature* **1996**, *382*, 607–609.

(2) Alivisatos, A. P.; Johnsson, K. P.; Peng, X.; Wilson, T. E.; Loweth, C. J.; Bruchez, M. P.; Schultz, P. G. *Nature* **1996**, *382*, 609−611.
(3) Leunissen, M. E.; Dreyfus, R.; Sha, R.; Seeman, N. C.; Chaikin, P. M. *J. Am. Chem. Soc.* **2010**, *132*, 1903−1913.
(4) Storhoff, J. J.; Elghanian, R.; Mucic, R. C.; Mirkin, C. A.; Letsinger, R. L. *J. Am. Chem. Soc.* **1998**, *120*, 1959−1964.
(5) Park, S.-J.; Taton, T. A.; Mirkin, C. A. *Science* **2002**, *295*, 1503−1506.
(6) Taton, T. A.; Mirkin, C. A.; Letsinger, R. L. *Science* **2000**, *289*, 1757−1760.
(7) Cao, Y. C.; Jin, R.; Mirkin, C. A. *Science* **2002**, *297*, 1536−1540.
(8) Rosi, N. L.; Giljohann, D. A.; Thaxton, C. S.; Lytton-Jean, A. K. R.; Han, M. S.; Mirkin, C. A. *Science* **2006**, *312*, 1027−1030.
(9) Nykypanchuk, D.; Maye, M. M.; van der Lelie, D.; Gang, O. *Nature* **2008**, *451*, 549−552.
(10) Park, S. Y.; Lytton-Jean, A. K. R.; Lee, B.; Weigand, S.; Schatz, G. C.; Mirkin, C. A. *Nature* **2008**, *451*, 553−556.
(11) Le, J. D.; Pinto, Y.; Seeman, N. C.; Musier-Forsyth, K.; Taton, T. A.; Kiehl, R. A. *Nano Lett.* **2004**, *4*, 2343−2347.
(12) Sharma, J.; Chhabra, R.; Liu, Y.; Ke, Y. G.; Yan, H. *Angew. Chem., Int. Ed.* **2006**, *45*, 730−735.
(13) Macfarlane, R. J.; Lee, B.; Jones, M. R.; Harris, N.; Schatz, G. C.; Mirkin, C. A. *Science* **2011**, *334*, 204−208.
(14) Leunissen, M. E.; Dreyfus, R.; Cheong, F. C.; Grier, D. G.; Sha, R.; Seeman, N. C.; Chaikin, P. M. *Nat. Mater.* **2009**, *8*, 590−595.
(15) Maye, M. M.; Nykypanchuk, D.; van der Lelie, D.; Gang, O. *J. Am. Chem. Soc.* **2006**, *128*, 14020−14021.
(16) Yurke, B.; Turberfield, A. J.; Mills, A. P.; Simmel, F. C.; Neumann, J. L. *Nature* **2000**, *406*, 605−608.
(17) Yan, H.; Zhang, X. P.; Shen, Z. Y.; Seeman, N. C. *Nature* **2002**, *415*, 62−65.
(18) Chakraborty, B.; Sha, R. J.; Seeman, N. C. *Proc. Natl. Acad. Sci. U.S.A.* **2008**, *105*, 17245−17249.
(19) Tian, Y.; Mao, C. D. *J. Am. Chem. Soc.* **2004**, *126*, 11410−11411.
(20) Dirks, R. M.; Pierce, N. A. *Proc. Natl. Acad. Sci. U.S.A.* **2004**, *101*, 15275−15278.
(21) Yin, P.; Choi, H. M. T.; Calvert, C. R.; Pierce, N. A. *Nature* **2008**, *451*, 318−322.
(22) Venkataraman, S.; Dirks, R. M.; Rothemund, P. W. K.; Winfree, E.; Pierce, N. A. *Nat. Nanotechnol* **2007**, *2*, 490−494.
(23) Zhang, D. Y.; Turberfield, A. J.; Yurke, B.; Winfree, E. *Science* **2007**, *318*, 1121−1125.
(24) Soloveichik, D.; Seelig, G.; Winfree, E. *Proc. Natl. Acad. Sci. U.S.A.* **2010**, *107*, 5393−5398.
(25) Franco, E.; Friedrichs, E.; Kim, J.; Jungmann, R.; Murray, R.; Winfree, E.; Simmel, F. C. *Proc. Natl. Acad. Sci. U.S.A.* **2011**, *108*, E784−E793.
(26) Qian, L. L.; Winfree, E. *Science* **2011**, *332*, 1196−1201.
(27) Zhang, D. Y.; Winfree, E. *J. Am. Chem. Soc.* **2009**, *131*, 17303−17314.
(28) Niemeyer, C. M.; Ceyhan, B.; Hazarika, P. *Angew. Chem., Int. Ed.* **2003**, *42*, 5766−5770.
(29) Liu, J. W.; Lu, Y. *Adv. Mater.* **2006**, *18*, 1667−1671.
(30) Jones, M. R.; Macfarlane, R. J.; Lee, B.; Zhang, J. A.; Young, K. L.; Senesi, A. J.; Mirkin, C. A. *Nat. Mater.* **2010**, *9*, 913−917.
(31) Dutta, P. K.; Varghese, R.; Nangreave, J.; Lin, S.; Yan, H.; Liu, Y. *J. Am. Chem. Soc.* **2011**, *133*, 11985−11993.
(32) Pal, S.; Deng, Z.; Wang, H.; Zou, S.; Liu, Y.; Yan, H. *J. Am. Chem. Soc.* **2011**, *133*, 17606−17609.